IOPscience iopscience.iop.org

Home Search Collections Journals About Contact us My IOPscience

Network theory approach for data evaluation in the dynamic force spectroscopy of biomolecular interactions

This content has been downloaded from IOPscience. Please scroll down to see the full text.

2010 EPL 89 68004

(http://iopscience.iop.org/0295-5075/89/6/68004)

View the table of contents for this issue, or go to the journal homepage for more

Download details:

IP Address: 147.91.1.45
This content was downloaded on 28/04/2014 at 15:52

Please note that terms and conditions apply.

A Letters Journal Exploring the Frontiers of Physics

March 2010

EPL, **89** (2010) 68004
doi: 10.1209/0295-5075/89/68004

www.epljournal.org

Network theory approach for data evaluation in the dynamic force spectroscopy of biomolecular interactions

J. Živković[1], M. Mitrović[3], L. Janssen[2], H. A. Heus[2], B. Tadić[3(a)] and S. Speller[1]

[1] *Scanning Probe Microscopy Group, Institute for Molecules and Materials, Radboud University Nijmegen, The Netherlands, EU*
[2] *Department of Biophysical Chemistry, Institute for Molecules and Materials, Radboud University Nijmegen, The Netherlands, EU*
[3] *Department of theoretical physics, Jožef Stefan Institute - Ljubljana, Slovenia, EU*

received 24 September 2009; accepted in final form 18 March 2010
published online 19 April 2010

PACS 82.37.Rs – Single molecule manipulation of proteins and other biological molecules
PACS 89.75.Hc – Networks and genealogical trees
PACS 02.70.Hm – Spectral methods

Abstract – Investigations of bonds between single molecules and molecular complexes by dynamic force spectroscopy are subject to large fluctuations at nanoscale and possible aspecific binding, which mask the experimental output. Big efforts are devoted to develop methods for the effective selection of the relevant experimental data, before the quantitative analysis of bond parameters. Here we present a methodology which is based on the application of graph theory. The force-distance curves corresponding to repeated pulling events are mapped onto their correlation network (mathematical graph). On these graphs the groups of similar curves appear as topological modules, which are identified using the spectral analysis of graphs. We demonstrate the approach by analyzing a large ensemble of the force-distance curves measured on: ssDNA-ssDNA, peptide-RNA (from HIV1), and peptide-Au surface systems. Within our data sets the methodology systematically separates subgroups of curves which are related to different types of intermolecular interactions and to spatial arrangements in which the molecules are brought together and/or pulling speeds. This demonstrates the sensitivity of the method to the spatial degrees of freedom, suggesting potential applications in the case of large molecular complexes and situations with multiple binding sites.

Copyright © EPLA, 2010

Introduction. – It has been recognized recently [1] that the signals generated at a single molecule (or another nanosize object) differ from signals obtained in large-scale systems consisting of ensemble of molecules. In particular, enhanced fluctuations, randomness and irreproducibility of the signals are observed in single-molecule measurements. A representative example is the mechanical signal generated in the dynamic force spectroscopy (DFS) of intermolecular bonds [2,3]. The force spectroscopy of individual molecules and molecular complexes has become a leading methodology for measuring biomolecular unbinding forces, which form the bases of biologically relevant molecular processes [4]. For instance, recently studied examples include measurements of fundamental biomolecular forces in DNA unzipping [5], ALCAM-ALCAM [6], peptide-antibody [7], RNA-protein [8] interactions, etc.

In a typical pulling experiment in DFS based on the atomic force microscopy, the ligand and receptor molecule are attached via polymer linkers on the AFM tip and the solid support (*e.g.*, glass, mica, gold surfaces). The molecules are brought close to each other for a certain contact time allowing them to form a bond and then pulled apart until the bond breaks. The process is repeated many times. In each pulling event, changes in the deflection of the AFM cantilever as a function of distance are measured. Knowing the spring constant of the cantilever, these data can be converted into distance-dependent forces, resulting in the so-called force-distance curves. From these curves different parameters can be obtained, such as the force needed to break a certain bond and the force loading rate. Further quantitative analysis of these data requires an elaborated theoretical framework [2] enabling the extraction of binding parameters, *i.e.*, potential barrier and the survival time. The applied force reduces the barrier

(a) E-mail: bosiljka.tadic@ijs.si

between the bound and dissociated states of the binding molecules, allowing one to estimate the force at which the barrier disappears and to measure the dissociation rate. Then the *natural* dissociation rate at vanishing force is extracted using an appropriate theoretical framework. Within the reaction-rate theory a unified formulation is currently available [9,10] for several types of interaction potentials, which also contains the classical model [2] as a special limit. Another direction of theoretical research, whereto also our work belongs, focuses on the nature of fluctuations (beyond the problem of signal-to-noise ratio) and suitable selection of the force-distance curves in different molecular systems. Curve selection represents an important step which *precedes* the quantitative analysis yielding the bonding parameters. The complexity of the problem arises from i) strong fluctuation in chemically rich and spatially extended molecular systems (see our discussion below), and ii) the large amount of data necessary to analyse. Hence, to sort the relevant data, both new concepts to treat the fluctuations properly as well as efficient computational approaches are needed. Recently two methods were proposed based on pattern recognition [11] and master-curve fitting [12].

The analytical expression for the profile of the force-distance curve is known in the case of a pulled linear polymer chain [13]. However, the data collected from the force spectroscopy experiments in molecular complexes (such as DNA-DNA, RNA-protein, ligand-receptor, etc.) often show very diverse profiles. In such (chemically) complex situations several binding events can occur simultaneously. For instance, an aspecific binding of RNA to the substrate or to the polymer linkers. Moreover, multiple bonds can be formed, which may result in many peaks per curve or larger detected forces. This makes force-distance curves difficult to sort and analyze on the basis of a single prototype profile, calling for more appropriate methods. It is generally accepted (see also discussion in [12]) that the force-distance curves originating from the same unbinding process share strong similarity.

In this work we present a new approach for systematic selection of groups of mutually similar force-distance curves and demonstrate it on a mixed set of force-distance curves from different experiments. Our methodology is based on the theory of complex networks and their spectral analysis [14–16]. Mapping multichannel datasets onto a graph representation has proved as a useful tool [17] in the analysis of many complex dynamical systems, for example stock-market time series [18], gene-expression signals [19,20], neural activity signals [21–23], temperature records in climate [24], and information traffic [25]. Compared to these examples, where the time-series are measured at each unit of an extended interacting system, our approach here is to map the force-distance signal measured in repeated experiments on the same molecular complex with many degrees of freedom. To demonstrate our approach, we analyze a large dataset consisting of force-distance curves measured under different conditions

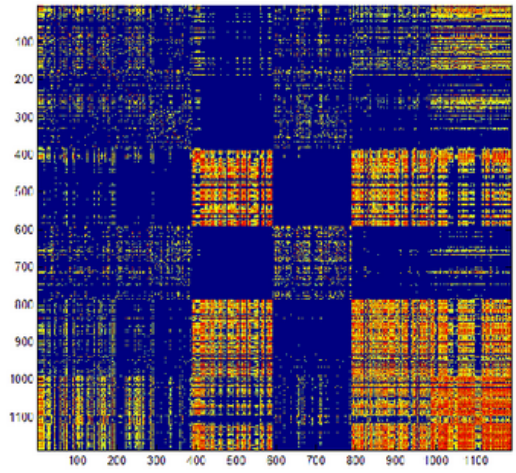

Fig. 1: (Colour on-line) Correlation matrix of different types of force curves, described in the text. Color intensity from blue (low) to red (high) indicates the strength of correlation C_{ij} between pairs of curves. Shown are correlations $C_{ij} > 0.5$ after matrix filtering.

on RNA-peptide complex (from HIV1), a set of curves from ssDNA-ssDNA binding and two control sets. The filtered correlation matrix mapped onto a binary graph exhibits modularity, with the subgraphs of nodes (curve index) grouped according to their similarity over the entire datasets. We then look at the force curves in each subgraph and find the underlying reasons for their clustering.

Description of the experimental data. – We created the correlation matrix from all pairs of $N = 1188$ force curves, that were pre-processed in the following way: We remove the contact part which mainly carries information on the cantilever. Further we applied an offset to shift the interaction free part of the curves to the baseline, and only the part where interactions are expected was kept (first 200 nm). Curves for the correlation matrix were selected from four different experiments with two different experimental setups. The experimental setups differ in the number of flexible linkers to couple molecules to the surface and the cantilever: either both molecules were coupled to the cantilever/surface via PEG spacers or one was coupled directly to the gold surface and the other to the cantilever via PEG spacer (NHS-PEG-MAL, length ~ 40 nm). In the correlation matrix (see fig. 1 and text below), from left-to-right, the first block (I) consists of 200 curves from measurements of the RNA-Rev peptide interaction (two linkers, velocity 581 nm/s); the second block (II) consists of 188 binding curves of RNA-Rev peptide in the presence of neomycin (two linkers, velocity 581 nm/s); the third block (III) contains 200 curves from RNA-Rev peptide interaction (one linker, velocity 2540 nm/s); the fourth block (IV) contains 200 curves measured on ssDNA-ssDNA interaction (with 30 complementary bp, two linkers, velocity 218 nm/s); the fifth block (V) has 200 curves of RNA-Rev peptide interaction (one linker, velocity 1160 nm/s), and

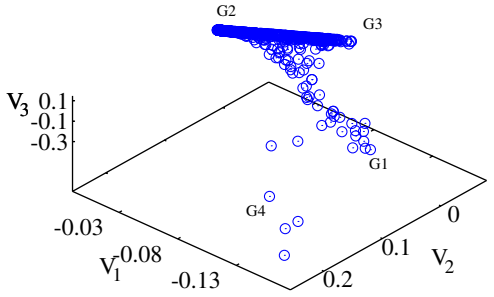

Fig. 2: (Colour on-line) Scatterplot of the eigenvectors V_1, V_2, V_3 of three lowest eigenvalues of the Laplacian operator (2) related to the full correlation matrix in fig. 1. Four branches are visible in this projection, marked as G_1, G_2, G_3, G_4.

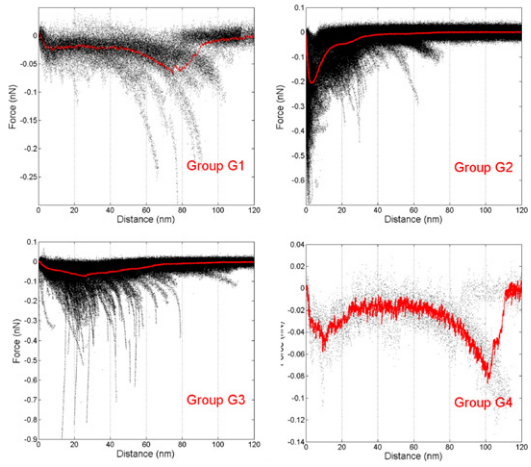

Fig. 3: (Colour on-line) Overlap plot of all curves belonging to the groups G_1, G_2, G_3, G_4 identified from the scatterplot in fig. 2.

the block (VI) consists of 200 curves of Rev peptide-Au interaction (one linker, velocity 1160 nm/s). Overlay of all curves used in this paper, grouped according to fig. 2, is shown in figs. 3.

Correlation matrix and its spectral analysis. – In our dataset consisting of $N = 1188$ force-distance curves, $\{f_i(x)\}$, $i = 1, 2, 3, \ldots, N$, each curve is identified by a uniquely defined index i, thus representing a separate pulling event. The elements of the correlation matrix C_{ij} are calculated as Pearson's correlation coefficient between each pair (i, j) of curves as follows:

$$C_{ij} = \frac{\sum_{i,j}[f_i(x) - \langle f_i \rangle][f_j(x) - \langle f_j \rangle]}{\sigma_i \sigma_j}, \qquad (1)$$

where the distance x is given by a discrete set of measured values, and σ_i, σ_j stand for the standard deviation of the force signal $f_i(x)$ and $f_j(x)$. In fig. 1 we show the correlation matrix of all force curves, after filtering out spurious correlations (the color map indicates values of the coefficients C_{ij}). For the filtering, we used the affinity transformation method [22,25], where the element is enhanced as $C_{ij} \to M_{ij} C_{ij}$ if the rows i and j correlate with the rest of the matrix in a similar way, yielding $M_{ij} \sim 1$, and diminished otherwise. The meta-correlation factor M_{ij} is computed as a Pearson's coefficient of the rearranged elements $\{C_{ij}, C_{i1}, \ldots, C_{ii-1}, C_{ii+1}, \ldots, C_{iN}\}$ and $\{C_{ji}, C_{j1}, \ldots, C_{jj-1}, C_{jj+1}, \ldots, C_{jN}\}$ without diagonal.

For further discussion we note that the matrix can be represented by a network (mathematical graph), where each matrix index $i = 1, 2, \ldots, N$ defines a network node and the matrix element C_{ij} —a link between nodes i and j. In our case the links are symmetrical $C_{ij} = C_{ji}$ by definition (1). Note that the matrix and network representations are formally equivalent. The network picture is suitable for visualization and topological interpretation. In particular, the matrix in fig. 1 makes a sparse network containing topological *modules*, *i.e.*, groups of nodes with strong connections inside the group and sparse connections between them. As the fig. 1 shows, correlations between different sets of data (blocks I through VI) shown as off-diagonal block-matrices can be as strong as correlations inside the same set (diagonal blocks). This means that the network modules may contain curves from different data blocks, suggesting their similarity over different experimental setups! In the following we apply the eigenvalue spectral methods to identify these modules.

Here we perform spectral analysis of the normalized Laplacian operator $\mathbf{L}$ related to the filtered correlation $\mathbf{C}$ in fig. 1, or more precisely, its binary form with the elements: $A_{ij} = 1$ whenever $C_{ij} > C_0$, or $A_{ij} = 0$ otherwise. The matrix elements of the Laplacian are given by [16,26]

$$L_{ij} = \delta_{ij} - \frac{A_{ij}}{\sqrt{q_i q_j}}, \qquad (2)$$

where q_i, q_j are the number of links at nodes i and j, respectively. Although the same conclusions can be reached using the adjacency matrix A_{ij} directly, the analysis of the Laplacian (2) is more convenient since its eigenvalue spectrum is limited in the range $\lambda_i \in [0, 2]$. Moreover, its *eigenvectors belonging to few lowest nonzero eigenvalues tend to localize along the network modules* [15,16]. This is a direct consequence of the orthogonality to the eigenvector belonging to zero eigenvalue of the Laplacian (or the largest eigenvalue of the adjacency matrix) which has all components positive (Perron-Frobenius theorem [27]). Precisely, the localization means that, among N components of the eigenvector, the nonzero (positive/negative) components have indexes which coincide with nodes in a network module (a detailed analysis of spectra in modular networks is given in [16]). This property of the eigenvectors we use to identify nodes in different modules.

Identification of modules: force-curves grouping. – When a modular structure occurs, the localization of eigenvectors belonging to the smallest nonzero eigenvalues is manifested in a *branched* pattern of the scatter plot

Table 1: Upper part: representative curves appearing at tips of four branches G_1, G_2, G_3, G_4 in the scatterplot in fig. 2 and their distribution over original blocks of data I through VI. Middle and bottom: further splitting of groups G_2 and G_3.

Block	I	II	III	IV	V	VI
G_1	5	9	0	16	0	0
G_2	51	28	177	0	181	148
G_3	60	68	0	135	1	7
G_4	4	0	1	0	0	0
G_2-g_1	5	1	3	0	35	22
G_2-g_2	0	0	45	0	7	0
G_2-g_3	20	10	5	0	3	21
G_3-g_1	5	6	0	24	1	0
G_3-g_2	24	9	0	24	0	5
G_3-g_3	18	15	0	28	0	1

in the space of these eigenvectors [16]. In fig. 2 we show the scatterplot of the eigenvectors (V_1, V_2, V_3) for three smallest nonzero eigenvalues of the Laplacian (2), related to the correlation matrix in fig. 1. In the scatterplot, each point carries one index, thus indicating one network node, that is a force curve index in our original dataset. The plot in fig. 2 shows four branches, marked as G_1, G_2, G_3, G_4, thus four groups of curves can be identified. The most representative curves in each group are those at the tips of branches with the most distinct curves situated at the opposite ends of the branches G_2 and G_3, whereas, the differences gradually diminishes closer to the center of the plot. By matching the indexes with curves in the original dataset, we identify representative curves at the tips of four branches (table 1). Overlay of all curves in the $G_1 \ldots G_4$ groups is shown in fig. 3. Heterogeneity of the curves in the block I, eventually splitting into two distinct groups, is compatible with the occurrence of weak correlations in the block after the filtering. Part of the curves from block I has strong correlation with the curves from block VI, which can be explained by the dominant adhesion peak and unspecific interaction of the peptide with the surface present in both data sets [28].

Each of the groups contains a number of curves from one or several blocks of the original datasets. Recalling the nature of the data in different blocks, we see that the module G_2 contains curves obtained predominantly on experimental setup with one PEG spacer (blocks III, V, and VI) and a fraction of data with two spacers (from blocks I and II) while *completely excluding* the DNA-DNA interactions (block IV). On the other hand, the module G_3 contains data from DNA-DNA interactions and a number of curves from Rev-RNA and blocked Rev-RNA with neomycin, all obtained with two spacers. G_1 has similar composition although it appears as a separate module, similar as the small group G_4. Note that these groups of curves show peaks at different regions of forces, cf. fig. 3, and occupy different areas in the force-distance plane (see rupture patterns below and supportive material [28]).

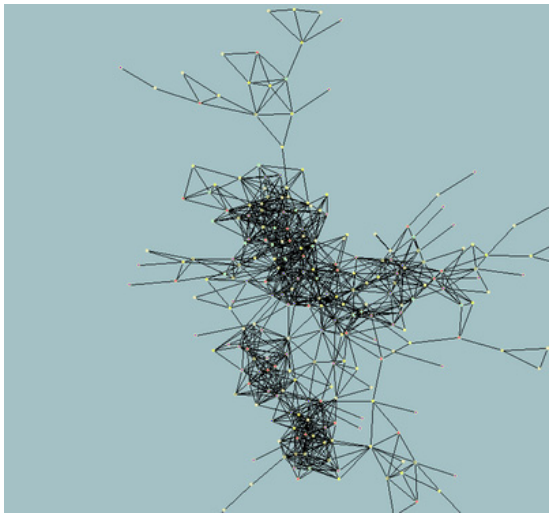

Fig. 4: (Colour on-line) Example of the correlation network constructed from the force curves in group G_2 from fig. 2, exhibiting modular structure. Shown are only links above the threshold $C_0 = 0.91$.

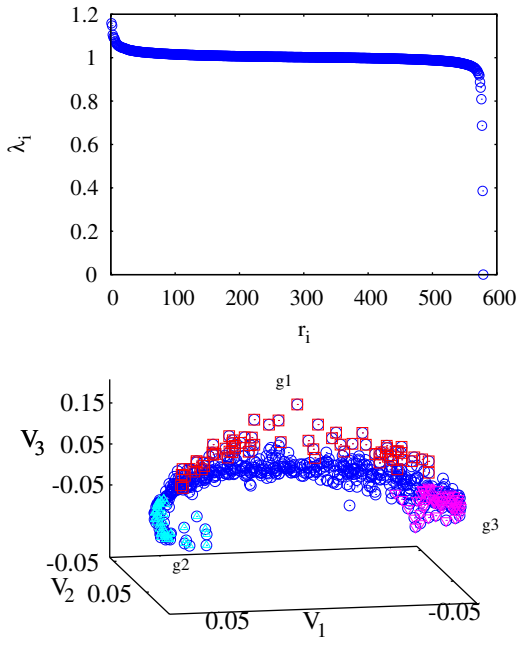

Fig. 5: (Colour on-line) For the branch G_2 of fig. 2: (top) the eigenvalue spectrum and (bottom) the scatterplot of three eigenvectors belonging to the lowest nonzero eigenvalues. Three subgroups are identified marked by g_1, g_2, g_3, see text for details.

We further analyze the group of curves in G_2 applying the same approach on the now reduced correlation matrix. The complete group consists of $N_2 = 597$ curves. The correlation network of these curves, shown in fig. 4, exhibits a modular structure, suggesting that smaller subgroups of the group G_2 can be identified. The eigenvalues of the Laplacian related to this correlation matrix are shown in the ranking order in fig. 5, top

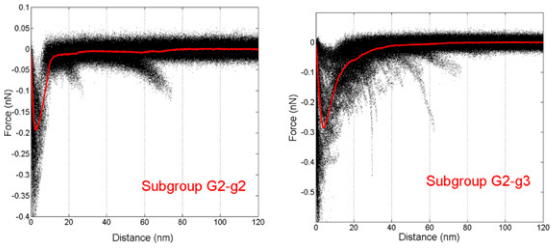

Fig. 6: (Colour on-line) Overlay of the selected force curves of low- and high-velocity associated to ends of the scatterplot ring in fig. 5.

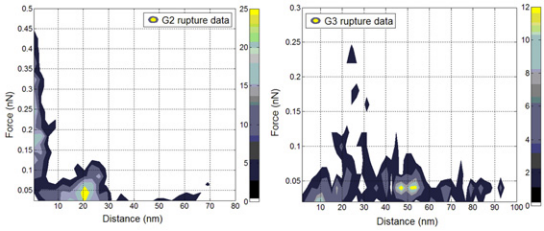

Fig. 7: (Colour on-line) Contour plots showing different patterns of the rupture events in the force-distance plane for two groups of curves selected by our methodology.

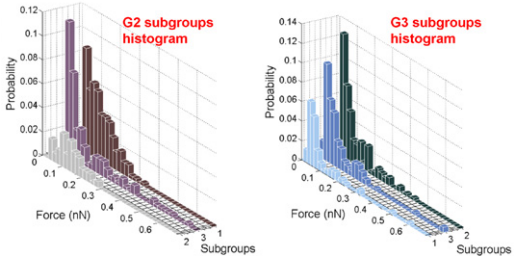

Fig. 8: (Colour on-line) Histograms of the rupture forces for three selected subgroups of FD curves of the groups G_2 (left) and G_3 (right).

panel. Compatible with the network modularity in fig. 4 is the appearance of three eigenvalues in the gap between $\lambda = 0$ and the main part of the spectrum. The corresponding scatterplot in the space of three eigenvectors belonging to these eigenvalues is also shown in fig. 5, bottom panel. In this case similarity between points, forming a half-helmet in (V_1, V_2, V_3) space, is stronger compared to fig. 2, however, groups can be identified by the end points of the half-ring in the horizontal plane and points with largest vertical distance, marked as g_1, g_2, g_3 and different symbols (colors) in fig. 5.

The identity of these curves with respect to the original datasets is also indicated in table 1, middle part. As mentioned above, curves in the large group G_2 are on Rev peptide binding, whereas, their subgroups appear to stem from experiments with different pulling velocities: G_2-g_1 consists mostly of curves in blocks V and VI, measurements at velocity of 1160 nm/s, while the groups G_2-g_2 and G_2-g_3 at two ends of the semi-ring contains curves measured at highest (2540 nm/s) and lowest (581 nm/s) velocity. In the experiment, measurements at different velocities and correct assignments of the curves are important for the extrapolation of bonding parameters to zero force values. The pulling velocity affects both force loading rate and the disruption force. Within our methods selected groups of high- and low-velocity curves, G_2-g_2 and G_2-g_3, respectively, are shown in fig. 6. Similar analysis of the group G_3 (not shown) leads to the curves identified in the lower part of the table 1. Here data contain three molecular systems (DNA-DNA, Rev-RNA, and Rev-RNA-with-neomycin) with multiple rupture profiles (see fig. 7) from the setup with two spacers and low velocity. Much larger mixing between the experimental situations in this group indicates either increased amount of aspecific binding or a dominant role of spacers.

The quality of the clustering is further demonstrated in figs. 7 and 8, where we show the rupture patterns in the force-distance plane and the histograms of the rupture forces for curves in groups G_2 and G_3 selected by our methodology. Different rupture patterns shown in fig. 7 suggest that not only different values of the most probable rupture forces are measured, *i.e.*, 0.141 ± 0.013 nN and 0.0337 ± 0.0012 nN, respectively for G_2 and G_3, but also indicate different distances where these events occur. It is remarkable that G_2 contains curves with the peptide interactions, while excluding the DNA-DNA curves consequently. Moreover, the identified subgroups, for instance within G_2, represent three distinct areas of the rupture pattern (supportive material [28]). Accordingly, the corresponding histograms for these subgroups of curves, shown in fig. 8, indicate different values of the most probable rupture forces, *i.e.*, 0.066 ± 0.006, 0.135 ± 0.008, and 0.038 ± 0.004. These results are estimates of the forces involved in these diverse sets of data used here for the demonstration. Further testing of the algorithm on data from a single experiment is necessary to optimize the clustering parameters such that different interactions, possible different binding sites or even different binding modes can be identified.

Conclusions. – We have shown that stochastic signals of different molecular systems (peptide-RNA, DNA-DNA) measured by dynamic force spectroscopy can be effectively selected according to their similarities. Our methodology uses the signal's relevant correlation matrix mapped onto a mathematical graph. Then using the eigenvalue spectral analysis of these graphs the groups of similar curves are detected, which appear as topological modules on them. We have shown that strong regularities in groupings of the force curves occur (and can be effectively used for the signal evaluation), based on the pulling speeds and experimental setup and even the type of the interaction measured, supported by different rupture patterns in the force-distance plane. This methodology represents a step towards clustering of the data according to the force-distance curve profiles, revealing a higher

sensitivity to certain bond natures than current standard methods. Along with the specificity, the numerical routines involved in our approach are faster compared to the classical pattern recognition methods [11]. Within a selected subgroup of FD curves further pre-processing, *e.g.*, with master-curve fitting [12], could be incorporated and increase the selectivity of our method. Improved efficiency of this approach is expected in particular in the case of larger molecular complexes and situations where distinction between many different binding sites is desired.

* * *

Work supported by the FP6 project Functional and Structural Genomics on Viral RNA: FSG-V-RNA, the FP7 project CYBEREMOTIONS, and the Nanotechnology programme of the Ministry of Economic Affairs, NanoNed (The Netherlands) and the national program P1-0044 (Slovenia). JŽ also thanks for the hospitality during her stay at the J. Stefan Institute, Ljubljana.

REFERENCES

[1] Barkai E., Brown F., Orrit M. and Yang H., *Theory and Evaluation of Single-Molecule Signals* (World Scientific, Singapore) 2008.
[2] Evans E. and Ritchie K., *Biophys. J.*, **72** (1997) 1541.
[3] Strunz T., Oroszlan K., Schäfer R. and Güntherodt H., *Proc. Natl. Acad. Sci. U.S.A.*, **96** (1999) 11277.
[4] Zlatanova J., Lindsay S. and Leuba S., *Prog. Biophys. Mol. Biol.*, **74** (2000) 37.
[5] Koch S. and Wang M., *Phys. Rev. Lett.*, **91** (2003) 028103.
[6] te Riet J., Zimmerman A., Cambi A., Joosten B., Speller S., Torensma R., van Leeuwen F., Figdor C. and de Lange F., *J. Cell Sci.*, **120** (2007) 3965.
[7] Sulchek T., Friddle R., Langry K., Lau E., Albrecht H., Ratto V., DeNardo S., Colvin M. and Noy A., *Proc. Natl. Acad. Sci. U.S.A.*, **102** (2005) 16638.
[8] Fuhrmann A., Schoening J., Anselmetti D., Staiger D. and Ros R., *Biophys. J.*, **96** (2009) 5030.
[9] Dudko O., Hummer G. and Szabo A., *Phys. Rev. Lett.*, **96** (2006) 108101.
[10] Dudko O., Hummer G. and Szabo A., *Proc. Natl. Acad. Sci.*, **105** (2008) 15755.
[11] Marsico A., Labudde D., Sapra T., Muller D. and Schroeder M., *Bioinformatics*, **23** (2005) e231.
[12] Fuhrmann A., Anselmetti D. and Ros R., *Phys. Rev. E*, **77** (2006) 031912.
[13] Bustamante C., Marko J. and Smith S., *Science*, **265** (1994) 1599.
[14] Boccaletti S., Latora V., Moreno Y., Chavez M. and Hwang D. U., *Phys. Rep.*, **424** (2006) 175.
[15] Donetti L. and Muñoz M. A., *J. Stat. Mech. Theor. Exp.*, **10** (2004) P10012.
[16] Mitrović M. and Tadić B., *Phys. Rev. E*, **80** (2009) 026123.
[17] Baruchi I., Grossman D., Volman V., Shein M., Hunter J., Towle V. and Ben-Jacob E., *Chaos*, **16** (2006) 015112.
[18] Mantegna R. N., *Eur. Phys. J. B*, **11** (1999) 193.
[19] Živković J., Tadić B., Wick N. and Thurner S., *Eur. Phys. J. B*, **50** (2006) 255.
[20] Živković J., Mitrović M. and Tadić B., *Correlation Patterns in Gene Expression along the Cell Cycle of Yeast, Springer Series: Studies in Computational Intelligence,* Vol. **207** (Springer) 2009, pp. 23–34.
[21] Zemanova L., Zhou C. and Kurths J., *Physica D*, **224** (2006) 202.
[22] Baruchi I. and Ben-Jacob E., *Neuroinformatics*, **2** (2004) 333.
[23] Graben R., Zhou C., Thiel M. and Kurths J., *Lectures in Supercomputational Neuroscience: Dynamics in Complex Brain Networks (Understanding Complex Systems)* (Springer-Verlag, Berlin, Heidelberg) 2008.
[24] Yamasaki K., Gozolchiani A. and Havlin S., *Prog. Theor. Phys. Suppl.*, **179** (2009) 178.
[25] Tadić B. and Mitrović M., *Eur. Phys. J. B*, **71** (2009) 631.
[26] Samukhin A. N., Dorogovtsev S. N. and Mendes J. F. F., *Phys. Rev. E*, **77** (2008) 036115–+.
[27] Godsil C. and Royle G., *Algebraic Graph Theory* (Springer-Verlag, Berlin, Heidelberg) 2001.
[28] Živković J., Jansen L., Alvarado F., Heus H., Tadić B. and Speller S., *Supportive material epl09: Rupture patterns in force-distance plane*, `http://www-f1.ijs.si/~tadic/supp-mat/supp_epl09.pdf` (2009).